

Influence of spatial dispersion on plasmons along graphene sheets

© M.V. Davidovich

Saratov National Research State University,
410012 Saratov, Russia

e-mail: davidovichmv@info.sgu.ru

Received December 21, 2023

Revised December 21, 2023

Accepted December 21, 2023

Taking into account the spatial dispersion and tensor conductivity of graphene, the dispersion equations of plasmons along single sheets of graphene and two sheets, including those located on a substrate, are obtained. A method for determining the dispersion equation for an arbitrary number of sheets and layers is proposed. For slow plasmons with a large distance between the sheets, the equations split into two for single sheets. When the conduction tensor is reduced to a diagonal form, the equations are simplified, and when the plasmon moves along one of the axes, the equations for E-plasmons and H-plasmons that coincide with those known for scalar conductivity decay. Plasmons up to optical and near UV frequencies are considered and numerically investigated, the influence of spatial dispersion is revealed. Plasmons with a deceleration of more than 106 were found.

Keywords: graphene, multilayered structures, plasmons, Cubo–Greenwood conductivity, Green’s function method.

DOI: 10.21883/0000000000

Introduction

Surface plasmons (SP) or plasmon polaritons along single graphene sheets were studied in works [1,2], as well as along two graphene sheets in [3], and then in [4]. At the same time, graphene was considered, neglecting spatial dispersion (SD), as a 2D material with scalar surface conductivity, which is true at not very large decelerations (wave vector components) and also at sufficiently low frequencies. Typically, SP are considered up to the THz range inclusive. However, in the IR, optical and especially in the UV ranges, the SD should be taken into account, and accordingly the tensor conductivity of graphene, which depends on the wave vector, should be taken into account. In strong fields, one should take into account the nonlinear properties of graphene and plasmon polaritons in it [5]. There are reviews on SP in graphene [6–8], in which graphene is described by scalar conductivity. A number of works have considered multilayer structures with graphene and metasurfaces [7–12]. The influence of a weak SD on the SP in graphene was considered in the work [13] based on the method of dyadic Green’s functions (GF) and Sommerfeld-type integrals. It has been shown that SD are significant above the THz range.

In this work, we generalize the approach of work [13] to multilayer structures with graphene sheets in several planes, considering the linear conductivity of graphene as a linear response to a tangential electric field, and accordingly looking for linear electromagnetic waves (SP) along the surfaces by solving dispersion equations (DE). In this case, we neglect Van der Waals and other interactions between graphene sheets and substrates, i.e., we use the conductivity model of suspended graphene in a vacuum. In the absence of substrates, this model is valid for

distances between graphene sheets that significantly exceed the characteristic size of 0.335 nm for a graphene bilayer and α -graphite. Otherwise, the dispersion in graphene changes significantly [14,15]. Among the SP, slow waves that are attenuated from surfaces, i.e., having a surface character, are important. In addition to them, fast leaky (antisurface according to the classification of the work [16]) waves are potential, which are emitted at an angle of leakage to the surface [17]. Dissipation leads to a change from a non-dissipative surface wave to a dissipative surface leaky wave, and strictly at the cutoff frequency, at which the wave travels at the speed of light and without dissipation, and all its energy propagates in a vacuum. Meanwhile, the inflowing wave above the cutoff becomes outflowing below it [16,17]. In an infinite waveguide structure, the fields of such waves would increase with distance from the surface [16]. The conductivity of graphene is complex, therefore SP are complex dissipative. For such waves, it is interesting the opportunity of the existence of branches with reverse SP, which are not determined by negative anomalous dispersion, i.e. the presence of a falling section on the dispersion branch $\omega = \omega(k')$: $\partial_k \omega(k') < 0$, where k' — any real part of the components (k_x, k_y) of the wave vector $k = k' - ik''$ [17]. It is the inverse SP that are determined by the negative sign of the value $k'(\omega)k''(\omega)$, which is equivalent to the movement of energy (decay) opposite to the movement of the phase. A more complex way of determining the inverse SP — defining the Poynting vector \mathbf{S} . The condition $\mathbf{S}k < 0$ is equivalent to $\mathbf{k}'(\omega)\mathbf{k}''(\omega) < 0$. The slow surface SP, which weakly decay along the motion along the surface are of great interest. They can be excited by laser beams and electron flows, and in the latter case, based on the interaction of the SP with the beam, it is possible

to create traveling wave amplifiers of the TWT [18] type, starting from the THz range, where the deceleration of the SP is already significant. Additional amplification in the THz range can be provided by laser pumping, creating a negative differential conductivity of graphene by irradiation with a laser at the optical pumping frequency [9,19]. Thus, the structures with SP studied in this work are important for a number of applications. In particular, optically active (pumped) structures can be used as antennas (emitters) of leaking waves and elements of active devices for generating and amplifying waves. In the works [7–12,19–28] and a number of others, SP in heterostructures and metasurfaces with graphene, including hyperbolic metamaterials and metasurfaces [29–34], are reviewed. It is important to take into account dissipation [35–42], since it determines the maximum deceleration. For graphene, the most rigorous account of SD requires integration over the entire Brillouin zone [24]. This, in particular, leads to a significant change in the dielectric permittivity (DP) and dispersion of bulk SP in multilayer graphene [23,24], as well as in graphene-based metamaterials.

1. Problem statement and model

We consider a single graphene sheet and a double graphene sheet with a distance $d \gg 0.335$ nm between them. At a smaller distance, there is Van der Waals interaction, the band structure of graphene changes, a small energy slit appears, and the graphene bilayer should be described by surface conductivity corresponding to the changed band structure [14,15]. For generality, we review sheets in an infinite ideal transparent medium with DP ε , and then the case $\varepsilon = 1$ corresponds to vacuum. Another case under consideration — sheets are located on a substrate of thickness d . A thin substrate of thickness $d \ll \lambda/\sqrt{\varepsilon_d}$ can be approximately taken into account based on two-sided boundary conditions by introducing surface conductivity $\sigma_d = i\omega\varepsilon_0(\tilde{\varepsilon}-1)d = \sigma_d = ik_0d\eta_0(\tilde{\varepsilon}-1)$, $\eta_0 = \sqrt{\varepsilon_0/\mu_0}$. Indeed, the substrate is described by the volume polarization current density $\mathbf{j}(\mathbf{r}) = i\omega\varepsilon_0(\varepsilon-1)[\mathbf{x}_0E_x(\mathbf{r}) + \mathbf{y}_0E_y(\mathbf{r}) + \mathbf{z}_0E_z(\mathbf{r})]$. By neglecting the $E_z(\mathbf{r})$ component and averaging, the surface conductivity of the thin dielectric layer $\sigma_d(\omega) = i\xi_d\eta_0$ can be introduced. This allows to simplify the problem using the Green's function (GF) $G(\mathbf{r}) = (4\pi r)^{-1} \exp(-ik_0r)$, $r = |\mathbf{r}| = \sqrt{x^2 + y^2 + z^2}$. For homogeneous substrates and multilayer structures, the transfer matrix method can be used. Accounting for SD requires the use of fourth-order transfer matrices. In the work in the general case of multilayer structures with homogeneous layers, such an approach based on fourth-order transfer matrices has been developed. The model consists of expressing the surface current density of each layer through the tangential electric field $\mathbf{J}_n(\omega, \mathbf{k}) = \hat{\sigma}(\omega, \mathbf{k})\mathbf{E}_\tau(\omega, \mathbf{k}, z_n)$ and matching the fields at the interfaces. The wave is assumed to be flat, the structures are infinite in x, y , so spectral amplitudes are used

everywhere. DE take the form of nonlinear transcendental equations, the search for roots of which is performed iteratively and leads to the dependencies $\mathbf{k} = \mathbf{f}(\omega)$.

2. Intradband conductivity of graphene

The crystal structure of graphene is determined by the translation vectors $\mathbf{e}_1 = (\sqrt{3}a/2, -a/2)$, $\mathbf{e}_2 = (0, a)$ and the corresponding reciprocal lattice vectors $\mathbf{g}_1(4\pi/(\sqrt{3}a),)$, $\mathbf{g}_2 = (2\pi/(\sqrt{3}a), 2\pi/a)$. The band structure of graphene was obtained by diagonalization of the Hamiltonian in the tight-binding approximation and is presented in a number of works [43–51]. The tensor dynamic surface conductivity of graphene relates the surface current density $\mathbf{J}(\omega, \mathbf{k})$ to the tangential (index τ) electric field of the plane wave $\mathbf{E}(t, \mathbf{r}) = \mathbf{E}(\omega, \mathbf{k}) \exp(i\omega t - i\mathbf{k}\mathbf{r}_\tau - ik_z z)$: $\mathbf{J}(\omega, \mathbf{k}) = \hat{\sigma}(\omega, \mathbf{k})\mathbf{E}_\tau(\omega, \mathbf{k})$. It is the sum of the intraband and interband parts: $\hat{\sigma}(\omega, \mathbf{k}) = \hat{\sigma}^{\text{intra}}(\omega, \mathbf{k}) + \hat{\sigma}^{\text{inter}}(\omega, \mathbf{k})$, $\mathbf{r}_\tau = x\mathbf{x}_0 + y\mathbf{y}_0$, $\mathbf{k} = k_x\mathbf{x}_0 + k_y\mathbf{y}_0$, $k = \sqrt{k_x^2 + k_y^2}$ [1,43,44]. Here $\mathbf{E}_\tau(\omega, \mathbf{r}_\tau) = \mathbf{z}_0\mathbf{E}(\omega, \mathbf{r})\mathbf{z}_0$, $z = 0$ — tangential electric field. It can also be found as $\mathbf{E}_\tau(\omega, \mathbf{r}) = \mathbf{E}(\omega, \mathbf{r}) - \mathbf{z}_0(\mathbf{z}_0\mathbf{E}(\omega, \mathbf{r}))$. Dependence on \mathbf{k} means spatial dispersion, and on frequency ω — frequency (time) dispersion. For plane wave diffraction $k_0^2 = \omega^2/c^2 = \mathbf{k}^2 + k_z^2$, and the value of $k^2 = \mathbf{k}^2 \leq k_0^2$ is limited. When the SP propagates, the problem of eigenvalues arises, and due to dissipation its solution has the form $\mathbf{k}(\omega) = \mathbf{n}' - i\mathbf{n}'' = \mathbf{k}'(\omega) - i\mathbf{k}''(\omega)$, and it is possible to introduce a complex vector refraction index $\mathbf{n}(\omega) = \mathbf{n}'(\omega) - i\mathbf{n}''(\omega) = \mathbf{k}(\omega)/k_0$, and the deceleration coefficient $n = |\mathbf{n}'(\omega)|$ can be either greater than unity (slow SP) or less than unity (fast SP). In this case, the propagation of the SP is significantly (especially in the region of large decelerations) influenced by the dissipation $\mathbf{n}'' = \mathbf{k}''(\omega)/k_0$, which can be directed both in the direction of the propagation of the SP, and in the opposite direction [17,33,34]. With a very decelerated SP $\mathbf{n}' \gg 1$, the role of SP dispersion is significant. To determine the intraband surface conductivity, we will use the relation [51]:

$$\mathbf{J}(\omega, \mathbf{k}) = 2 \frac{e}{(2\pi)^2} \int_{BZ} (\mathbf{v}^+ f_{FD}^+(\mathbf{q}, \mathbf{E}_\tau) - \mathbf{v}^- f_{FD}^-(\mathbf{q}, \mathbf{E}_\tau)) d^2\mathbf{q}. \quad (3)$$

In it, the signs + and – indicate the values for the upper (electron) and lower (hole) subbands conjugated at the Dirac points, the two corresponds to the factor g , the Fermi–Dirac $f_{FD}^\pm(\mathbf{q}, \mathbf{E}_\tau)$ distribution densities are used, perturbed by a plane wave of the electric field. The tangential electric field $\mathbf{E}_\tau(\omega, \mathbf{k})$ interacts with graphene, which is associated with the normal component $E_z = \mathbf{z}_0\mathbf{E}(\omega, \mathbf{k}, k_z) = |\mathbf{E}(\omega, \mathbf{k}, k_z)| \sqrt{1 - k^2/k_0^2}$, $k^2 = \mathbf{k}^2$, $\mathbf{k} = x\mathbf{x}_0 + y\mathbf{y}_0$ — -dimensional wave vector in the graphene plane, $k_0^2 = k^2 + k_z^2$. In the general case, the connection (3) with the field $\mathbf{E}_\tau(\omega, \mathbf{k})$ is nonlinear [5]. In weak fields, the disturbances are small, and, according to the Kubo model,

there is a linear relationship between the current and field components. Expressions for the perturbed PD distributions are obtained from the RTA (relaxation-time approximation) approximation, or in the Bhatnagar–Gross–Crook (BGC) approximation of the solution to the kinetic equation. The latter is more preferable since it satisfies charge conservation. In this approximation $\tilde{\sigma}^{\text{intra}}(\omega, \mathbf{k}) = \tilde{\sigma}^e(\omega, \mathbf{k}) + \tilde{\sigma}^h(\omega, \mathbf{k})$, and the space-time spectral functions have the following representations [51]:

$$\begin{aligned}\sigma_{xx}^{e,h}(\omega, \mathbf{k}) &= \\ &= \frac{\tilde{\sigma}_{xx}^{e,h}(\omega, \mathbf{k}) + k_y(\tilde{\sigma}_{xy}^{e,h}(\omega, \mathbf{k})d_y^{e,h} - \tilde{\sigma}_{yx}^{e,h}(\omega, \mathbf{k})d_x^{e,h})}{1 + k_x d_x^{e,h} + k_y d_y^{e,h}}, \\ \sigma_{xy}^{e,h}(\omega, \mathbf{k}) &= \\ &= \frac{\tilde{\sigma}_{xy}^{e,h}(\omega, \mathbf{k}) + k_y(\tilde{\sigma}_{xx}^{e,h}(\omega, \mathbf{k})d_y^{e,h} - \tilde{\sigma}_{yy}^{e,h}(\omega, \mathbf{k})d_x^{e,h})}{1 + k_x d_x^{e,h} + k_y d_y^{e,h}}, \\ \sigma_{yx}^{e,h}(\omega, \mathbf{k}) &= \\ &= \frac{\tilde{\sigma}_{yx}^{e,h}(\omega, \mathbf{k}) + k_x(\tilde{\sigma}_{xx}^{e,h}(\omega, \mathbf{k})d_x^{e,h} - \tilde{\sigma}_{yy}^{e,h}(\omega, \mathbf{k})d_y^{e,h})}{1 + k_x d_x^{e,h} + k_y d_y^{e,h}}, \\ \sigma_{yy}^{e,h}(\omega, \mathbf{k}) &= \\ &= \frac{\tilde{\sigma}_{yy}^{e,h}(\omega, \mathbf{k}) + k_x(\tilde{\sigma}_{xy}^{e,h}(\omega, \mathbf{k})d_x^{e,h} - \tilde{\sigma}_{xy}^{e,h}(\omega, \mathbf{k})d_y^{e,h})}{1 + k_x d_x^{e,h} + k_y d_y^{e,h}},\end{aligned}\quad (4)$$

These relations include components of tensors $\tilde{\sigma}_{xx}^{e,h}$, vectors $\mathbf{d}^{e,h}$ and scalars $F_{e,h}$, defined as [51]:

$$\begin{aligned}|\tilde{\sigma}^{e,h}(\omega, \mathbf{k}, \mu)| &= \frac{-ie^2}{8k_B T \pi^2} \\ &\times \int_{BZ} \frac{\mathbf{v}^\pm(\mathbf{q}) \otimes \mathbf{v}^\pm(\mathbf{q}) d^2 q}{\cosh^2\left(\frac{E^\pm(\mathbf{q}) - \mu^\pm}{2k_B T}\right) (\omega - i\omega_c - \mathbf{k}\mathbf{v}^\pm(\mathbf{q}))}, \\ \mathbf{d}^{e,h}(\omega, \mathbf{k}, \mu) &= \frac{-i\omega_c}{\omega F_{e,h}(\omega, \mathbf{k})} \\ &\times \int_{BZ} \frac{\mathbf{v}^\pm(\mathbf{q}) d^2 q}{\cosh^2\left(\frac{E^\pm(\mathbf{q}) - \mu^\pm}{2k_B T}\right) (\omega - i\omega_c - \mathbf{k}\mathbf{v}^\pm(\mathbf{q}))}, \\ F_{e,h}(\omega, \mathbf{k}, \mu) &= \int_{BZ} \frac{d^2 q}{\cosh^2\left(\frac{E^\pm(\mathbf{q}) - \mu^\pm}{2k_B T}\right) (\omega - i\omega_c - \mathbf{k}\mathbf{v}^\pm(\mathbf{q}))},\end{aligned}\quad (5)$$

where the integrals use integration over the upper subband (electron conduction band) and over the lower subband (for holes). In these integrals the following is denoted: $\mathbf{v}^\pm(\mathbf{q}) = \hbar^{-1} \nabla_{\mathbf{q}} E^\pm(\mathbf{q})$ — velocities of charge carriers in subbands, $\mathbf{q} = q_x \mathbf{x}_0 + q_y \mathbf{y}_0$ — two-dimensional vector associated with the $\mathbf{p} = \hbar \mathbf{q}$ pulse, ω_c — collision frequency. As for the latter, it is usually considered small and is required for the correct calculation of integrals (bypassing the poles). However, in reality in graphene, especially with doping,

electron-hole scattering, it can be significant, while depending on frequency (photon energy), temperature, and can be different in subbands. For the velocity components we have

$$\begin{aligned}v_x^\pm(\mathbf{q}) &= \mp \frac{2\sqrt{3}v_F \gamma_0}{E^\pm(\mathbf{q})} \sin\left(\frac{3q_x a}{2}\right) \cos\left(\frac{\sqrt{3}q_y a}{2}\right), \\ v_y^\pm(\mathbf{q}) &= \mp \frac{v_F \gamma_0}{E^\pm(\mathbf{q})} \sin\left(\frac{\sqrt{3}q_y a}{2}\right) \\ &\times \left[\cos\left(\frac{3q_x a}{2}\right) + 2 \cos\left(\frac{\sqrt{3}q_y a}{2}\right) \right].\end{aligned}$$

In the center of the Brillouin zone $v_x^\pm(0) = v_y^\pm(0) = 0$, while $E^\pm(0) = \pm 3\gamma_0$. At the Dirac point $\mathbf{K}' = 2\pi(1, 1/\sqrt{3})/(3a)$ (Fig. 1) we have $E^\pm(\mathbf{K}') = 0$, and for the velocity components we obtain an uncertainty of 0/0. The same occurs at point $\mathbf{K} = 2\pi(1, -1/\sqrt{3})/(3a)$. The uncertainty is revealed by expanding the energy in the vicinity of the Dirac points [51] $E^\pm(\mathbf{q}) = \pm \hbar v_F |\mathbf{q} - \mathbf{q}_F|$, where $v_F = \sqrt{3}\gamma_0 a / (2\hbar)$ — Fermi velocity. Thus, $v_F \approx c/300$ — maximum media velocity.

Numerical calculation of integrals (5) when iteratively determining the roots of the differential equation requires large computational costs. Integrals (5) can be calculated by expanding in terms of the small parameter $k v_F / (c k_0)$, the smallness of which is achieved with decelerations $n = k/k_0 \ll c/v_F = 300$. In this case, relations (5) can be transformed. For example, for scalar values we have

$$\begin{aligned}F_{e,h}(\omega, k_x, 0, \mu) &= \frac{1}{\omega - i\omega_c} \int_{BZ} \frac{dq_x dq_y}{\cosh^2((E^\pm(\mathbf{q}) - \mu)/(2k_B T))} \\ &+ \frac{1}{(\omega - i\omega_c)^2} \int_{BZ} \frac{[k_x v_x^\pm(\mathbf{q}) + k_y v_y^\pm(\mathbf{q})] dq_x dq_y}{\cosh^2((E^\pm(\mathbf{q}) - \mu)/(2k_B T))}.\end{aligned}$$

For tensor components in the numerators, additional factors appear $v_\alpha^\pm v_\beta^\pm$, and for vector components v_α^\pm , $\alpha, \beta = x, y$. A more rigorous approach requires numerical integration [24]. People are often interested in the movement of the SP along one of the coordinate axes, for example, with $k_y = 0$. In this case the relations are simplified. Let us review the first zone in Fig. 1. We will integrate over the upper right triangle. The integral over the first variable is taken within the limits of $0 \leq q_x \leq q_{0x} = 2\pi/(3a)$. The integral over the second variable is taken within the limits of $0 \leq q_y \leq q_x q_{0y}/q_{0x} = q_x/(\sqrt{3})$. Taking the limits $-q_x/(\sqrt{3}) \leq q_y \leq q_x/(\sqrt{3})$, we obtain the integral over the upper and lower right-angled triangles, i.e. over the right equilateral triangle. The integral over the left of such a triangle is obtained by changing the signs of the variables and the limits, so the result should be doubled. Thus, the result of integration over two triangles is

$$\int_{2\Delta} (dq_x dq_y) = 2 \int_0^{2\pi/(3a)} dq_x \int_{-q_x/\sqrt{3}}^{q_x/\sqrt{3}} (dq_y).$$

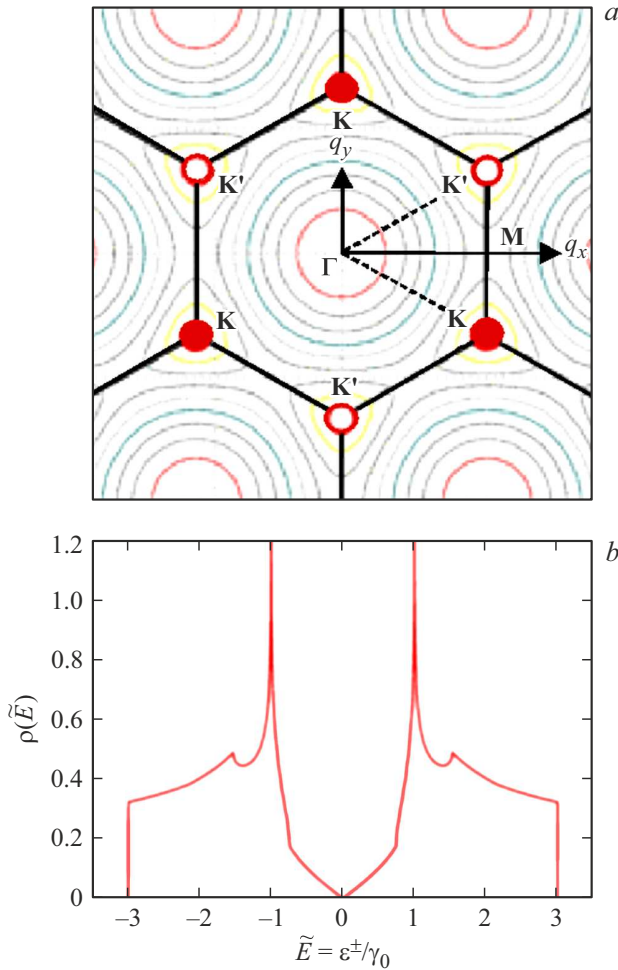


Figure 1. First Brillouin zone, isoenergy lines and integration over triangles (a) and density of states in graphene per lattice cell depending on the normalized energy $\tilde{E} = \varepsilon^\pm(\mathbf{k})/\gamma_0$ at $\gamma_0 = 0$ (b).

Due to the symmetry of the Brillouin zone (Fig. 1), we can write

$$\int_{BZ} (dq_x dq_y) = 6 \int_0^{2\pi/(3a)} dq_x \int_{-q_x/\sqrt{3}}^{q_x/\sqrt{3}} (dq_y). \quad (6)$$

The specified result can be obtained by replacing variables by rotating the coordinate system by angle $\pi/3$. It is convenient to perform numerical integration based on such a formula. Another potential way of integrating — over energy and one of the momentum components. In pure graphene at zero temperature, the one-electron density of states per cell at the Fermi level is zero, and its dependence on energy is plotted in Fig. 2 (see [47]). It was obtained by calculating the spectral integral over the Brillouin zone for a finite lifetime of quasiparticles (excitations) $\tau_l = 1/\omega$:

$$\rho_0(\omega\hbar) = -\frac{2\text{Im}}{4\pi^2} \int_{BZ} \sum_{l=\pm} \frac{dk_x dk_y}{\hbar\omega - \varepsilon^l(k_x, k_y) + i\hbar\omega_c}.$$

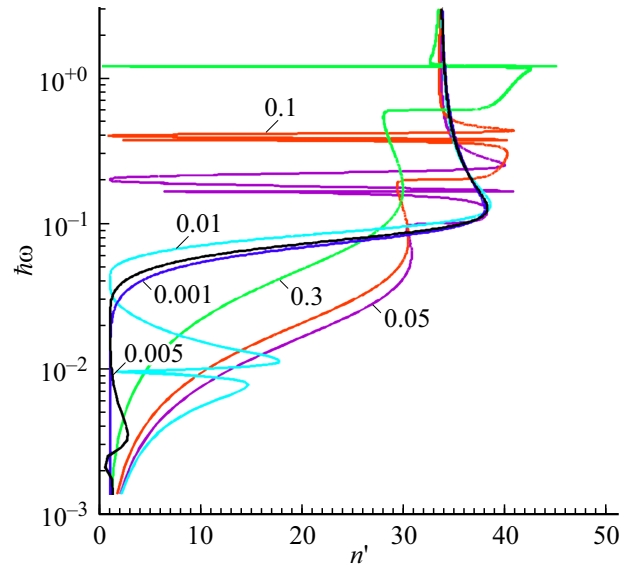


Figure 2. E-SP dispersion (dependence of $\omega\hbar$, eV, on the deceleration $n' = k'_x/k_0$) taking into account SD for different values of the chemical potential μ_c (shown in eV), $\omega_c = 10^{12}$ GHz.

Let us find the local density of states in k -space. We then obtain [47,48]:

$$G(q_x) = \frac{g_s}{(2\pi/a)^2} \int_{BZ} dq_x dq_y = \frac{4g_s}{(2\pi/a)^2} \int_0^{k_x} dk'_s \times \int_0^{4\pi/(3\sqrt{3}a) - q_x/\sqrt{3}} dk'_y = \frac{4g_s q_x (4\pi/(3a) - q_x/2)}{(2\pi/a)^2 \sqrt{3}},$$

or $G(q_x) = (\pi^{-2} 3^{-1/2}/6) q_x a (8\pi - 3q_x a)$. Here we took $g_s = 2$, went to the integral over the quarter zone and quadrupled the result. Full density is $\tilde{G} = 2/(3\sqrt{3})$. Since the size of the hexagon edge of the zone is $4\pi/(3\sqrt{3}a)$, and the total area of the zone is $8\pi^2/(3\sqrt{3}a^2)$, taking into account the area per state $(2\pi/a)^2$ and the factor $g_s = 2$, we obtain the same result for \tilde{G} . The local density of states is

$$g(q_x) = (d/dq_x)G(q_x) = \frac{4g_x (4\pi/(3a) - q_x)}{(2\pi/a)^2 \sqrt{3}}.$$

Here $0 < k_x < 2\pi/(3a)$. Approximating ρ based on the graph in Fig. 2, we can write

$$g(q_x) = 2 \int_0^{\tilde{E}} \rho(E) dE. \quad (7)$$

B (6) we count the energy from the bottom of the valence band (Fermi level). Linear approximation allows you to calculate the integral and express the energy as the root of the quadratic equation explicitly through $g(q_x)$,

i.e. obtain the function $\tilde{E} = \Phi(q_x)$. I.e. it can be considered independent variables \tilde{E} and q_y . Similarly, \tilde{E} and q_x can be taken as independent variables. In this case,

$$\int_{\tilde{BZ}} (dq_x dq_y) = - \int_{-3}^3 \int_{2\pi/(3a)}^{2\pi/(3a)} \int_{-3}^3 d\tilde{E} dq_x, \quad (8)$$

$$Y(q_x, \tilde{E}) = \frac{-\cos(3q_x a/2) + \sqrt{\cos^2(3q_x a/2) + \tilde{E}^2 - 1}}{2},$$

$$q_y = \frac{2}{\sqrt{3}a} \arccos(Y(q_x, \tilde{E})).$$

When w is squared, the number of roots doubles, so in (8) one sign of the root is taken. Indeed, with $q_x = 0$, $w = 3$ we get the correct result $q_y = 0$. At the point \mathbf{K} we have $w = 0$, and accordingly $q_y = -2\pi/(3\sqrt{3}a)$. At the point $(0, 4\pi/(3\sqrt{3}a))$ there are $w = 0$ and $q_y = 4\pi/(3\sqrt{3}a)$ again. It should be noted that the density of states at nonzero chemical potentials for epitaxial graphene can differ significantly, therefore integration (6) is preferable to (8).

3. Interband conductivity of graphene

Interband conductivity is associated with the absorption (or emission) of an $2\hbar\omega$ energy quantum carrier and its symmetrical transition to another subband. For example, an electron in the valence band with energy $-\hbar\omega$ (relative to UV) goes to the conduction band with energy $\hbar\omega$. Interband conductivity is determined by the expression [1]

$$\sigma_{\alpha\beta}^{\text{inter}}(\omega) = \frac{-ie^2\hbar}{S} \sum_{\mathbf{q}, l \neq l'} \frac{f_{FD}(E_{\mathbf{q}l}) - f_{FD}(E_{\mathbf{q}l'})}{E_{\mathbf{q}l} - E_{\mathbf{q}l'} - \hbar(\omega - i\omega_c)} \times \frac{\langle \mathbf{q}, l | \hat{v}_\alpha | \mathbf{q}, l' \rangle \langle \mathbf{q}, l' | \hat{v}_\beta | \mathbf{q}, l \rangle}{E_{\mathbf{q}l} - E_{\mathbf{q}l'}}. \quad (9)$$

Here $f_{FD}(E_{\mathbf{q}l})$ — PD distribution, $\hat{v}_\alpha = V\hat{\sigma}_\alpha$ — velocity operator, $\psi = |\mathbf{q}, l\rangle$ — wave function, $\hat{\sigma}_\alpha$ — Pauli matrix, $l = 1, 2$ corresponds to the lower (hole) and upper (electronic) subbands (i.e. $l = 2$ — electron conduction band), $\alpha, \beta = x, y$, $E_{\mathbf{q}l} = (-1)^l \hbar v_F q$, $q = \sqrt{q_x^2 + q_y^2}$, $\hat{H}(\hat{\mathbf{p}}) = v_F \hat{\sigma}_\alpha \hat{p}_\alpha$, $S = \sqrt{3}a_0^2/4 = a^2/(4\sqrt{3}) = 0.0524 \text{ nm}^2$. The result (9) corresponds to the normal wave incidence $\mathbf{k} = 0$.

In the work [43], based on the temperature GF method, a representation of the conductivity $\sigma_{\alpha,\beta}(\omega, \mathbf{k}) = i\sigma_0 (S_{\alpha\beta}^{\text{intra}}(\omega, \mathbf{k}) + S_{\alpha\beta}^{\text{inter}}(\omega, \mathbf{k}))$ (the sign of the

imaginary unit is changed) was obtained in the form

$$S_{\alpha\beta}^{\text{intra}}(\omega, \mathbf{k}) = \frac{4}{\pi^2} \sum_{l=1,2} \times \int \frac{v^\alpha v^\beta [f_{FD}(\varepsilon_l(\mathbf{p}_-)) - f_{FD}(\varepsilon_l(\mathbf{p}_+))]}{[\varepsilon_l(\mathbf{p}_+) - \varepsilon_l(\mathbf{p}_-)] [\omega - \varepsilon_l(\mathbf{p}_+) + \varepsilon_l(\mathbf{p}_-)]} d^2 p,$$

$$S_{\alpha\beta}^{\text{inter}}(\omega, \mathbf{k}) = \frac{8\omega}{\pi^2} \times \int \frac{v_{12}^\alpha v_{21}^\beta [f_{FD}(\varepsilon_1(\mathbf{p}_-)) - f_{FD}(\varepsilon_2(\mathbf{p}_+))]}{[\varepsilon_2(\mathbf{p}_+) - \varepsilon_1(\mathbf{p}_-)] \{\omega^2 - [\varepsilon_2(\mathbf{p}_+) - \varepsilon_1(\mathbf{p}_-)]^2\}} d^2 p.$$

In it, $l = 1, 2$ corresponds to the conduction band of electrons and the valence band, respectively, i.e. $\varepsilon_1(\mathbf{p}) = \varepsilon^+(\mathbf{p})$, $\varepsilon_2(\mathbf{p}) = \varepsilon^-(\mathbf{p})$, $\varepsilon_l(\mathbf{p}_\pm) = \varepsilon_l(\mathbf{p}) \pm \mathbf{p}_k \omega/2$, where $\mathbf{p}_k = \hbar\mathbf{k}$ — photon momentum, $\mathbf{p} = \hbar\mathbf{q}$, v^α — matrix element of the carrier velocity operator between states in one zone, v_{12}^α — matrix element of the carrier velocity operator between states in different zones. Further, the result in [43] was obtained for the dispersion $\varepsilon_l(\mathbf{p}_\pm) = v_F |\mathbf{p} \pm \hbar\mathbf{k}/2|$. For strong SD $\omega\hbar \ll kv_F$ and $\omega\hbar \ll k_B T$ we found $\sigma_\perp^{\text{inter}} = \sigma_\parallel^{\text{inter}}$ and

$$S_{\alpha\beta}^{\text{inter}}(\omega, k) = -i\delta_{\alpha\beta} \frac{2\omega}{\pi} \times \begin{cases} \frac{\hbar}{4k_B T k v_F} \ln(4k_B T / (\hbar k v_F)), & \omega \ll kv_F \ll k_B T / \hbar, \\ (k v_F)^{-1}, & \omega \ll T \ll kv_F. \end{cases}$$

In fact, summation in (9) is integration over two subbands. In the limit $k \rightarrow 0$ and taking into account the main linear contribution to the dispersion $E^\pm(\mathbf{q}) \approx \pm \hbar v_F |\mathbf{q} - \mathbf{q}_F|$ in the vicinity of the Dirac points (or $E^\pm(\mathbf{q}') = \pm \hbar v_F q'$), integrals of type (6) are reduced to expressions

$$\sigma^{\text{intra}}(\omega, \omega_c, \mu_c, T) = \frac{ie^2}{\pi\hbar^2(\omega - i\omega_c)} \times \int_0^\infty (\partial_\varepsilon f_{FD}(\varepsilon) - \partial_\varepsilon f_{FD}(-\varepsilon)) \varepsilon d\varepsilon, \quad (10)$$

$$\sigma^{\text{inter}}(\omega, \omega_c, k, \mu_c, T) = \frac{-ie^2(\omega - i\omega_c)}{\pi\hbar^2} \times \int_0^\infty \left[\frac{f_{FD}(-\varepsilon + k\hbar v_F/2)}{(\omega - i\omega_c - kv_F/2)^2 - \frac{4\varepsilon^2}{\hbar^2}} - \frac{f_{FD}(\varepsilon - k\hbar v_F/2)}{(\omega - i\omega_c + kv_F/2)^2 - \frac{4\varepsilon^2}{\hbar^2}} \right] d\varepsilon, \quad (11)$$

in which $f_{FD}(\varepsilon) = [\exp((\varepsilon - \mu_c)/(k_B T)) + 1]^{-1}$ — equilibrium function PD. In the works [2,44,51] these integrals are given at $k = 0$ in (11), i.e. without taking into account SD. Integral (10) at temperatures on the order of room temperature and below is calculated with good

accuracy in the form [2,44]

$$\begin{aligned}\sigma^{\text{intra}}(\omega, \omega_c, \mu_c, T) &= \frac{k_B T (e^2/\hbar) \varphi(\mu_c, T)}{\pi \hbar \omega_c (1 + i\omega/\omega_c)} \\ &= \frac{4\sigma_0 k_B T \varphi(\mu_c, T)}{\pi \hbar \omega_c (1 + i\omega/\omega_c)},\end{aligned}\quad (12)$$

$$\varphi(\mu_c, T) = \ln \left(2 \cosh \left(\frac{\mu}{2k_B T} \right) \right). \quad (13)$$

As for the integral (11), then for $k_B T \ll \mu_c$, $k_B T \ll \hbar\omega$, $k = 0$ it was calculated in the work [44]

$$\sigma^{\text{inter}}(\omega, \omega_c, \mu_c, T) \approx \frac{-i\sigma_0}{\pi} \ln \left(\frac{2|\mu_c| - (\omega - i\omega_c)\hbar}{2|\mu_c| + (\omega - i\omega_c)\hbar} \right). \quad (14)$$

In this case, in the integral (11) we can replace all functions f_{FD} by units at the lower limit $|\mu_c|$ of the integral, from which we obtain formula (14). For $\mu_c = 0$, (14) implies $\sigma^{\text{inter}} = \sigma_0 = e^2/(4\hbar)$, and (24) — $\sigma^{\text{intra}} = 0$. The dimensionless quantum conductivity of graphene $\xi_0 = \sigma_0 \eta_0 = \pi \alpha_0 = 0.0229$ can be expressed through the fine structure constant $\alpha_0 = 1/137$. These formulas are valid up to frequencies that satisfy the condition $\hbar\omega < 3 \text{ eV}$. Higher in the UV, photoionization of carbon atoms occurs first with the breaking of π bonds, and then other bonds, and then for conductivity the plasma quantum model of 2D electron gas should be used.

Formula (14) is not accurate even at room temperature at low electrochemical potentials and low frequencies even at $k = 0$. The most effective way is to numerically calculate the integral (11). Since the dispersion equation (DE) for the SP should be solved iteratively, the numerical calculation of the integrals is inconvenient, and it is desirable to have analytical expressions taking into account the SD. Let us introduce for further purposes the dimensionless chemical potential $\alpha = \mu_c/(k_B T)$ and the complex frequency $\beta = \hbar(\omega - i\omega_c)/(2k_B T)$. If $\alpha \sim 1$ or more, then $\varphi(\mu_c, T) \approx \alpha/2$. In the work [51] based on formulas (4) and (5) in the first approximation, the form of tensor conductivity of graphene was obtained taking into account the SD for intraband conductivity:

$$\begin{aligned}\sigma_{xx}(\omega, \omega_c, \mathbf{k}) &= \sigma^{\text{intra}} \left[1 + \frac{v_F^2}{4(\omega - i\omega_c)^2} \left(3 - \frac{2i}{\omega/\omega_c} \right) k_x^2 \right. \\ &\quad \left. + \frac{v_F^2}{4(\omega - i\omega_c)^2} k_y^2 \right] + \sigma^{\text{inter}}(k),\end{aligned}\quad (15)$$

$$\sigma_{xy}(\omega, \omega_c, \mathbf{k}) = \sigma^{\text{intra}} \left[\frac{v_F^2}{2(\omega - i\omega_c)^2} k_x k_y \right], \quad (16)$$

$$\begin{aligned}\sigma_{yy}(\omega, \omega_c, \mathbf{k}) &= \sigma^{\text{intra}} \left[1 + \frac{v_F^2}{4(\omega - i\omega_c)^2} \left(3 - \frac{2i}{\omega/\omega_c} \right) k_y^2 \right. \\ &\quad \left. + \frac{v_F^2}{4(\omega - i\omega_c)^2} k_x^2 \right] + \sigma^{\text{inter}}(k).\end{aligned}\quad (17)$$

The frequency dependence of scalar values has been omitted for brevity. The formulas are correct for relatively small \mathbf{k} , corresponding to decelerations significantly less than 300, i.e. the additions to the units in square brackets are small. These additions for (15) at $\omega_c = 0$ can be represented in the form $\delta\sigma^{\text{intra}} = (3/4)(n_x/300)^2 + (n_y/300)^2/4 \ll 1$. Here $\mathbf{n} = \mathbf{k}/k_0$ — vector deceleration coefficient. Formula (15) is deficient and the next term should be $(\delta\sigma^{\text{intra}})^2$. According to (15) – (17), SD increases the components of intraband conductivity, which leads to a limitation of the deceleration of the slow E-SP and to a slight increase in the deceleration of the H-DP. SD for interband conductivity was not reviewed in [51]. Let us calculate (11) by expanding in terms of the small parameter kv_F/β , taking into account only the linear term:

$$\sigma^{\text{inter}}(\beta, \alpha, k) = \sigma^{\text{inter}}(\beta, \alpha, 0) + \sigma^{(1)}(\beta, \alpha) kv_F/(\omega - i\omega_c).$$

We consider $k\hbar v_F/2 \ll \mu_c$, i.e. $\alpha \gg kv_F/\omega$. This allows us to believe in the functions of the PD $k = 0$. However, we will also take these linear terms into account. With linear dispersion used, the right-hand sides in (15) and (17) are isotropic. Interband conductivity with $E^\pm(\mathbf{q}') = \pm\hbar v_F q'$ dispersion is also isotropic. In the low SD approximation, integral (11) can be transformed using $f_{FD}(\pm\varepsilon \mp k\hbar v_F/2) \approx f_{FD}(\pm\varepsilon) \mp k\hbar v_F/2 \partial_\varepsilon f_{FD}(\pm\varepsilon)$ and the relations

$$\begin{aligned}&\int_0^\infty \frac{f_{FD}(\pm\varepsilon)}{\hbar^2(\omega - i\omega_c \mp kv_F/2)^2 - 4\varepsilon^2} d\varepsilon \\ &= \frac{1}{4\hbar} \int_0^\infty \frac{f_{FD}(\pm\varepsilon)}{\hbar(\omega - i\omega_c \mp kv_F/2) - 2\varepsilon} \frac{d\varepsilon}{\varepsilon} \\ &\quad - \frac{1}{4\hbar} \int_0^\infty \frac{f_{FD}(\pm\varepsilon)}{\hbar(\omega - i\omega_c \mp kv_F/2) + 2\varepsilon} \frac{d\varepsilon}{\varepsilon},\end{aligned}$$

$$\begin{aligned}&\int_0^\infty \frac{f_{FD}(\pm\varepsilon)}{\omega - i\omega_c \mp kv_F/2 - 2\varepsilon/\hbar} \frac{d\varepsilon}{\varepsilon} \approx \int_0^\infty \frac{f_{FD}(\pm\varepsilon)}{(\omega - i\omega_c - 2\varepsilon/\hbar)} \\ &\quad \times \left[1 \pm \frac{kv_F/2}{(\omega - i\omega_c - 2\varepsilon/\hbar)} \right] \frac{d\varepsilon}{\varepsilon}.\end{aligned}$$

The logarithmic singularities at zero of the set of integrals are eliminated. Let us first review the term $\sigma^{\text{inter}}(\omega, \omega_c, 0) = -ie^2(\omega - i\omega_c)(I_- - I_+)/(\pi\hbar^2)$, represented by formula (11) at $k = 0$. Let us consider $\mu_c > 0$. Since $\exp(-(\varepsilon + \mu_c)/(k_B T)) < 1$, in the first integral the expansion can be carried out in a small parameter and one

term can be left:

$$\begin{aligned} I_- &= \frac{\hbar^2}{4} \int_0^\infty \frac{1 - \exp(-(\varepsilon + \mu_c)/(k_B T))}{[\hbar(\omega - i\omega_c)/2]^2 - \varepsilon^2} d\varepsilon \\ &= \frac{\hbar^2}{4} \int_0^\infty \frac{d\varepsilon}{[\hbar(\omega - i\omega_c)/2]^2 - \varepsilon^2} \\ &\quad - \frac{\hbar^2}{4} \int_0^\infty \frac{\exp(-(\varepsilon + \mu_c)/(k_B T))}{[\hbar(\omega - i\omega_c)/2]^2 - \varepsilon^2} d\varepsilon. \end{aligned}$$

The first integral on the right is equal to $i\pi/[\hbar(\omega - i\omega_c)]$, i.e. its contribution to the conductivity is σ_0 . We replace $x = (\varepsilon + \mu_c)/(k_B T)$ in the second one and integrate part by part:

$$\begin{aligned} \frac{\hbar^2}{4k_B T} \int_\alpha^\infty \frac{\exp(-x)}{\beta^2 - (x + \alpha)^2} dx &= \frac{\hbar^2}{4k_B T} \\ &\times \left[\frac{\exp(-\alpha)}{\beta^2 - 4\alpha^2} + \int_\alpha^\infty \frac{2 \exp(-x)}{[\beta^2 - (x + \alpha)^2]^2} x dx \right]. \end{aligned}$$

When discarding the integral on the right, this formula already has good accuracy if $\mu_c \geq k_B T$. Further refinement comes down to integration by parts. Re-integration gives

$$\begin{aligned} \frac{\hbar^2 \exp(-\alpha)}{4k_B T (\beta^2 - 4\alpha^2)} \left(1 + \frac{2\alpha}{\beta^2 - 4\alpha^2} \right) &+ \int_\alpha^\infty \frac{2 \exp(-x)}{[\beta^2 - (x + \alpha)^2]^2} \\ &\times \left(1 + \frac{2x^2}{[\beta^2 - (x + \alpha)^2]^2} \right) dx, \\ \int_\alpha^\infty \frac{2 \exp(-x)}{[\beta^2 - (x + \alpha)^2]^2} x dx &= \frac{2\alpha \exp(-\alpha)}{[\beta^2 - 4\alpha^2]^2} \\ &+ \int_\alpha^\infty \frac{2 \exp(-x)}{[\beta^2 - (x + \alpha)^2]^2} \left(1 + \frac{2x^2}{[\beta^2 - (x + \alpha)^2]^2} \right) dx, \end{aligned}$$

where the contribution from the integral on the right has the form

$$\frac{2 \exp(-\alpha)}{(\beta^2 - 4\alpha^2)^2} \left[1 + \frac{2\alpha^2}{(\beta^2 - 4\alpha^2)^2} \right]$$

and can be discarded along with the remaining integral as small. We will take it into account. Therefore:

$$\begin{aligned} I_-(\alpha, \beta) &\approx -\frac{\hbar^2}{4k_B T} \left[\frac{\exp(-\alpha)}{\beta^2 - 4\alpha^2} \left(1 + \frac{2(\alpha + 1)}{\beta^2 - 4\alpha^2} \right) \right. \\ &\quad \left. + \frac{4\alpha^2}{(\beta^2 - 4\alpha^2)^2} \right] - \frac{i\pi}{2\beta}. \end{aligned} \quad (18)$$

For the second integral, we divide the integration domain into two: $0 < \varepsilon < 2\mu_c$ and $2\mu_c < \varepsilon < \infty$, replacing

$x = (\varepsilon - \mu_c)/(k_B T)$. This results in

$$\begin{aligned} I_+ &= \frac{\hbar^2}{4k_B T} \int_{-\alpha}^\alpha \frac{dx}{[\beta^2 - (x + \alpha)^2](1 + \exp(x))} \\ &+ \frac{\hbar^2}{4k_B T} \int_\alpha^\infty \frac{\exp(-x) - \exp(-2x) - \exp(-3x) - \dots}{\beta^2 - (x + \alpha)^2} dx. \end{aligned} \quad (19)$$

Omitting intermediate calculations, we present the final result:

$$\begin{aligned} \sigma^{\text{inter}}(\omega, \omega_c, 0) &= \sigma_0 + \frac{i\sigma_0}{\pi} \left[\frac{4\beta \exp(-\alpha)}{\beta^2 - 4\alpha^2} \left(1 + \frac{3\alpha + 1}{\beta^2 - 4\alpha^2} \right) \right. \\ &+ \frac{2\alpha^2}{(\beta^2 - 4\alpha^2)^2} - \frac{\exp(-2\alpha)}{4} \left. \right] + \frac{1}{1 + \exp(\alpha/2)} \\ &\times \ln \left(\frac{\beta^2 + \alpha\beta - 2\alpha^2}{\beta^2 - \alpha\beta - 2\alpha^2} \right) + \frac{1}{1 + \exp(-\alpha/2)} \ln \left(\frac{\beta - \alpha}{\beta + \alpha} \right). \end{aligned} \quad (20)$$

This formula has significantly better accuracy than (14). At low temperatures $k_B T \ll \mu_c$ the values of α and β are large, with $\alpha/\beta = 2\mu_c/\hbar(\omega - i\omega_c)$, and depending on the frequency this ratio can be either large or small. We have $\sigma^{\text{inter}}(\omega, \omega_c, 0) \approx \sigma_0$ at high frequencies ($\omega \gg 2\mu_c/\hbar$). At low frequencies (but at $k_B T \ll \hbar\omega \ll 2\mu$) we have $\sigma^{\text{inter}}(\omega, \omega_c, 0) = -2i\sigma_0\beta/(\pi\alpha)$, i.e. this part of the conductivity is small in magnitude and is inductive. In this case, the real part due to interband transitions can be small negative. The effect of pumping with population inversion but at high optical frequencies is considered in works [9–12, 20–22]. Now $\sigma^{\text{inter}}(\beta, \alpha, k) = \sigma^{\text{inter}}(\beta, \alpha, 0) + \sigma^{(1)}(\beta, \alpha)k v_F/(\omega - i\omega_c)$, while the value $\sigma^{(1)}(\beta, \alpha) = \sigma_1^{(1)}(\beta, \alpha) + \sigma_2^{(1)}(\beta, \alpha)$ is divided into two parts: the first part includes the linear term in the expansion of the PD functions in the numerator, and the second contains the corresponding term in the expansion of the denominators. The first one is calculated simply and is equal to

$$\sigma_1^{(1)}(\beta, \alpha) = -\frac{ie^2\beta^2}{\pi\hbar(\beta^2 - \alpha^2)}.$$

The second one has the form

$$\begin{aligned} \sigma_2^{(1)}(\beta, \alpha) &= \frac{4i\sigma_0(\hbar\omega - i\hbar\omega_c)^3}{\pi} \\ &\times \int_0^\infty \frac{f_{FD}(-\varepsilon) + f_{FD}(\varepsilon)}{(\hbar\omega - i\hbar\omega_c - 2\varepsilon)^2(\hbar\omega - i\hbar\omega_c + 2\varepsilon)^2} d\varepsilon. \end{aligned} \quad (21)$$

It is convenient to write (21) as follows

$$I = \frac{2\pi\sigma_2^{(1)}(\beta, \alpha)}{i\sigma_0(\hbar\omega - i\hbar\omega_c)^2} = \int_0^\infty \frac{f_{FD}(-\varepsilon) + f_{FD}(\varepsilon)}{\varepsilon} \times \left[\frac{1}{(\hbar\omega - i\hbar\omega_c - 2\varepsilon)^2} - \frac{1}{(\hbar\omega - i\hbar\omega_c + 2\varepsilon)^2} \right] d\varepsilon.$$

Obviously, now

$$I = -8\pi i (k_B T)^2 \sigma_2^{(1)}(\beta, \alpha) / (\sigma_0 \beta^2)$$

and

$$I(\beta, \alpha, T) = I_1^+(\beta, \alpha, T) - I_1^-(\beta, \alpha, T),$$

where $I_1^+(\beta, \alpha, T) = I_1^-(-\beta, \alpha, T)$. Although the I_1^\pm integrals have a logarithmic singularity at zero, this singularity is eliminated in the full integral. The integral is calculated under the assumption $k_B T \ll \mu_c$, which is usually done at room temperature. To calculate the integral, we divide the integration interval into two: $(0, 2\mu_c)$, $(2\mu_c, \infty)$, we denote $\Omega = \hbar\omega - i\hbar\omega_c$ and use the identity

$$\frac{1}{\varepsilon(2\varepsilon \pm \Omega)^2} = \frac{1}{\varepsilon\Omega^2} - \frac{4\varepsilon \pm 4\Omega}{(2\varepsilon \pm \Omega)^2\Omega^2}.$$

It follows the division into simple fractions:

$$\frac{1}{\varepsilon(2\varepsilon - \Omega)^2} - \frac{1}{\varepsilon(2\varepsilon + \Omega)^2} = \frac{2}{(2\varepsilon - \Omega)^2\Omega} - \frac{2}{(2\varepsilon + \Omega)^2\Omega^2} + \frac{2}{(2\varepsilon + \Omega)\Omega^2} + \frac{2}{(2\varepsilon + \Omega)^2\Omega^2}.$$

For the second interval, the sum of the PD functions is equal to unity with high accuracy, so the result for it has the form

$$-\frac{1}{\Omega^2} \ln \frac{4\mu_c + \Omega}{4\mu_c - \Omega} + \frac{1}{\Omega} \frac{8\mu_c}{16\mu_c^2 - \Omega^2} = -\frac{1}{(2k_B T\beta)^2} \ln \frac{2\alpha + \beta}{2\alpha - \beta} + \frac{1}{(k_B T)^2\beta} \frac{\alpha}{4\alpha^2 - \beta^2}.$$

At high frequencies it is small. We calculate the first integral using the mean value theorem, taking the value at the midpoint $\varepsilon = \mu_c$ for the sum of the PD functions:

$$\tilde{\varphi}(\alpha) \int_0^{2\mu_c} \left(\frac{\varepsilon + \Omega}{(\varepsilon + \Omega/2)^2\Omega^2} - \frac{\varepsilon - \Omega}{(\varepsilon - \Omega/2)^2\Omega^2} \right) d\varepsilon.$$

Here $\tilde{\varphi}(\alpha) = 1/2 + 1/(1 + \exp(-2\alpha)) \approx 3/2$ — the value of the sum of the PD functions at the midpoint. The result has the form

$$\tilde{\varphi}(\alpha) \left(\frac{1}{(2k_B T)^2\beta^2} \ln \left(\frac{\beta + 2\alpha}{\beta - 2\alpha} \right) - \frac{\alpha}{(k_B T)^2(4\alpha^2 - \beta^2)\beta} \right).$$

At high frequencies it is also small. Thus, we obtain the value of the integral

$$I(\alpha, \beta) = \frac{\tilde{\varphi}(\alpha) - 1}{(k_B T)^2} \left(\frac{1}{4\beta^2} \ln \left(\frac{\beta + 2\alpha}{\beta - 2\alpha} \right) - \frac{\alpha/\beta}{4\alpha^2 - \beta^2} \right)$$

and have the final result

$$\sigma^{(1)}(\beta, \alpha) = -\frac{4i\sigma_0\beta^2}{\pi(\beta^2 - \alpha^2)} + \frac{i\sigma_0(\tilde{\varphi}(\alpha) - 1)}{\pi} \times \left(\frac{1}{2} \ln \left(\frac{\beta + 2\alpha}{\beta - 2\alpha} \right) - \frac{2\alpha\beta}{4\alpha^2 - \beta^2} \right). \quad (22)$$

At high frequencies $\beta \gg \alpha$, the contribution of the SD to the conductivity is inductive: $\sigma^{(1)}(\beta, \alpha) = -4i\sigma_0/\pi$. The maximum contribution from SD to conductivity will be at $\beta \approx 2\alpha$. Assuming $\beta = 2\alpha - i\beta''$ and considering α and β' to be large values, and β'' to be small, we obtain

$$\sigma^{(1)}(\beta, \alpha) = -\frac{16i\sigma_0\alpha^2}{3\pi} + \frac{i\sigma_0}{4\pi} \ln \left(\frac{4\alpha}{\beta''} \right) - \sigma_0 \left(\frac{1}{8} + \frac{\alpha}{\pi\beta''} \right).$$

At low losses, this part of the conductivity may have a large negative real part, which indicates the occurrence of non-equilibrium due to interband transitions. Its imaginary part can be either capacitive or inductive. The last case corresponds to very small losses. The contribution of SD to conductivity has the form $2\hbar k v_F k_B T \sigma^{(1)}(\beta, \alpha) / \beta$.

4. Dispersion equation based on the Green's function method

The vector potential created by the current densities of two graphene sheets on a thin substrate has the form

$$\mathbf{A}(x, y, z) = \int_{-\infty}^{\infty} \int_{-\infty}^{\infty} \left[G(\boldsymbol{\rho} - \boldsymbol{\rho}', 0) \mathbf{J}_1(\boldsymbol{\rho}') + G(\boldsymbol{\rho} - \boldsymbol{\rho}', d) \times \mathbf{J}_2(\boldsymbol{\rho}') + G(\boldsymbol{\rho} - \boldsymbol{\rho}', d/2) \mathbf{J}_d(\boldsymbol{\rho}') \right] dx' dy'. \quad (23)$$

We denote the two-dimensional vector $\boldsymbol{\rho} = \mathbf{x}_0x + \mathbf{y}_0y$. Determining the electric field

$$\mathbf{E}(\mathbf{r}) = (ik_0)^{-1} \eta_0 (\nabla \otimes \nabla + \hat{I}k_0) \mathbf{A}(\mathbf{r}),$$

we impose boundary conditions:

$$\begin{aligned} J_{1x}(x, y) &= \sigma_{xx} E_x(x, y, 0) + \sigma_{xy} E_y(x, y, 0), \\ J_{1y}(x, y) &= \sigma_{xy} E_x(x, y, 0) + \sigma_{yy} E_y(x, y, 0), \\ J_{2x}(x, y) &= \sigma_{xx} E_x(x, y, d) + \sigma_{xy} E_y(x, y, d), \\ J_{2y}(x, y) &= \sigma_{xy} E_x(x, y, d) + \sigma_{yy} E_y(x, y, d), \\ J_{dx}(x, y) &= \sigma_d E_x(x, y, d/2), \\ J_{dy}(x, y) &= \sigma_d E_y(x, y, d/2). \end{aligned} \quad (24)$$

Here $\eta_0 = \sqrt{\mu_0/\varepsilon_0} = 376.73 \Omega$, we consider the conductivity of graphene sheets to be identical and tensor, the sheets located at $z = 0$ (first) and $z = d$ (second), and the scalar surface conductivity of the substrate $\sigma_d = i\omega\varepsilon_0(\varepsilon - 1)d$ — located at $z = d/2$. The tensor differential operator has components $(\nabla \otimes \nabla)_{kl} = \partial_k \partial_l$, $k, l = x, y, z$. We express the field components through a tensor GF of the all-electric type $\hat{G}^{ee}(\mathbf{r}) = (-ik_0 \hat{I} + ik_0^{-1} \nabla \otimes \nabla) \eta_0 G(\mathbf{r})$. Next, we move from all coordinate relations in transverse coordinates to their spatial Fourier transforms, which allows to obtain algebraic relations. Therefore

$$\hat{G}^{ee}(\mathbf{r}) = \frac{\eta_0}{4\pi^2} \int_{-\infty}^{\infty} \int_{-\infty}^{\infty} \hat{g}(k_x, k_y) \times \exp(-ik_x x - ik_y y - ik_z |z|) dk_x dk_y, \quad (25)$$

$$\hat{g}(k_x, k_y) = -\frac{1}{2k_0 k_z} \begin{bmatrix} k_0^2 - k_x^2 & -k_x k_y \\ -k_x k_y & k_0^2 - k_y^2 \end{bmatrix}. \quad (26)$$

Here $k_z = \sqrt{k_0^2 - k_x^2 - k_y^2}$. If the SP is slow, then $\kappa_z = \sqrt{k_x^2 + k_y^2 - k_0^2} = ik_z$ should be taken. Therefore, it is convenient to introduce the function $\psi = \exp(-\kappa_z d/2)$. We will denote the field components as $E_{nx}(k_x, k_y)$, $E_{ny}(k_x, k_y)$, where $n = 1, 2$ correspond to graphene sheets, and $n = 3$ — to the substrate. It is possible to obtain a system of six algebraic equations for the components of the electric field or six components of the surface current densities. It is more convenient to write them through the surface current density components. In addition, it is convenient to introduce dimensionless (normalized) conductivities: $\hat{\xi} = \sigma \eta_0$, $\hat{\xi}_d = \sigma_d \eta_0$. The first equation in (3) corresponds to the equation

$$\begin{aligned} & [1 - \hat{\xi}_{xx} g_{xx}(\mathbf{k}) - \hat{\xi}_{xy} g_{xy}(\mathbf{k})] j_{1x}(\mathbf{k}) \\ & - [\hat{\xi}_{xx} g_{xy}(\mathbf{k}) + \hat{\xi}_{xy} g_{yy}(\mathbf{k})] j_{1y}(\mathbf{k}) \\ & - \psi^2 [\hat{\xi}_{xx} g_{xx}(\mathbf{k}) + \hat{\xi}_{xy} g_{xy}(\mathbf{k})] j_{2x}(\mathbf{k}) \\ & - \psi^2 [\hat{\xi}_{xx} g_{xy}(\mathbf{k}) + \hat{\xi}_{xy} g_{yy}(\mathbf{k})] j_{2y}(\mathbf{k}) \\ & - \psi [\hat{\xi}_{xx} g_{xx}(\mathbf{k}) + \hat{\xi}_{xy} g_{xy}(\mathbf{k})] j_{dx}(\mathbf{k}) \\ & - \psi [\hat{\xi}_{xx} g_{xy}(\mathbf{k}) + \hat{\xi}_{xy} g_{yy}(\mathbf{k})] j_{dy}(\mathbf{k}) = 0. \quad (27) \end{aligned}$$

To get the second equation, it is required to make the replacement $x \leftrightarrow y$. To get the third equation, it is required to make the replacement $1 \leftrightarrow 2$. The fourth equation can be obtained by appropriate replacements from the first or from the second. To obtain it from the second equation, we make the replacement $1 \leftrightarrow 2$ in it. The fifth equation has the form

$$\begin{aligned} & -2\hat{\xi}_d \psi g_{xx}(\mathbf{k}) j_{1x}(\mathbf{k}) - 2\hat{\xi}_d \psi g_{xy}(\mathbf{k}) j_{1y}(\mathbf{k}) \\ & - 2\hat{\xi}_d \psi g_{xx}(\mathbf{k}) j_{2x}(\mathbf{k}) - 2\hat{\xi}_d \psi g_{xy}(\mathbf{k}) j_{2y}(\mathbf{k}) \\ & + j_{dx}(\mathbf{k}) [1 - \hat{\xi}_d g_{xx}(\mathbf{k})] - j_{dy}(\mathbf{k}) \hat{\xi}_d g_{xy}(\mathbf{k}) = 0. \quad (28) \end{aligned}$$

The sixth equation is obtained from the fifth by replacement $x \leftrightarrow y$. Here $\mathbf{k} = \mathbf{x}_0 k_x + \mathbf{y}_0 k_y$. The DE of free waves (SP) is obtained by setting the determinant of the resulting system of linear homogeneous equations to zero. It is quite bulky. Simplification is obtained for slow SP and large d , when ψ^2 can be neglected in comparison with. In this case, we obtain the DE in the form that the fourth-order determinant is equal to zero. Strict consideration of a homogeneous substrate requires the use of a cross-linking method. For scalar conductivity it is quite simple [3]. For tensor conductivity of graphene, it is convenient to use fourth-order transfer matrices. Such matrices in optics are known as Berreman matrices [52]. When matching the components of four $u = (E_x, \eta_0 H_y, -E_y, \eta_0 H_x)$ vectors, the normalized matrix for graphene has the form

$$\hat{T}_\sigma = \begin{bmatrix} 1 & 0 & 0 & 0 \\ \hat{\xi}_{xy} & 1 & -\hat{\xi}_{yy} & 0 \\ 0 & 0 & 1 & 0 \\ \hat{\xi}_{xx} & 0 & -\hat{\xi}_{xy} & 1 \end{bmatrix} \quad (29)$$

and the matrix for the substrate is formed as

$$\hat{T}(d) = \begin{bmatrix} \hat{a}^e(d) + \hat{a}^h(d) & \hat{0} \\ \hat{0} & \hat{a}^e(d) + \hat{a}^h(d) \end{bmatrix}. \quad (30)$$

In it $\hat{0}$ — zero two-dimensional matrix, and two-dimensional matrices are designated

$$\hat{a}^{e,h}(d) = \begin{bmatrix} \cos(\tilde{d}_z d) & i\rho_{e,h} \sin(\tilde{k}_z d) \\ iy_{e,h} \sin(\tilde{k}_z d) & \cos(\tilde{k}_z d) \end{bmatrix}.$$

In them $\rho_{e,h} = y_{e,h}^{-1} = Z_{e,h}/\eta_0$, $\rho_e = \tilde{k}_e/(k_0 \varepsilon)$, $\rho_h = k_0/\tilde{k}_e$ — normalized characteristic impedances of E-waves and H-waves, $\tilde{k}_z = \sqrt{k_0^2 \varepsilon - k_x^2 - k_y^2}$. The DE is obtained by the method described in [17], in which the condition of either wave inflow (for a slow surface SP) or wave outflow (for a fast antisurface SP) is used. Such a DE has the form of a fourth-order determinant equal to zero. It can be reduced to a second-order determinant [17]. Next, for simplicity, we consider graphene sheets in an infinite dielectric. This case is obtained by replacing $k_0 \rightarrow k_0 \sqrt{\varepsilon}$ in all proportions, while $k_z \rightarrow \tilde{k}_z$, and \mathbf{J}_d should be omitted. In this case, the DE takes the form

$$\det \begin{bmatrix} \hat{I} - \hat{A}(\mathbf{k}) & -\psi^2(k) \hat{A}(\mathbf{k}) \\ -\psi^2(k) \hat{A}(\mathbf{k}) & \hat{I} - \hat{A}(\mathbf{k}) \end{bmatrix} = 0, \quad (31)$$

$$\hat{A}(\mathbf{k}) = \begin{bmatrix} \hat{\xi}_{xx} g_{xx} + \hat{\xi}_{xy} g_{xy} & \hat{\xi}_{xx} g_{xy} + \hat{\xi}_{xy} g_{yy} \\ \hat{\xi}_{yy} g_{xy} + \hat{\xi}_{xy} g_{xx} & \hat{\xi}_{yy} g_{yy} + \hat{\xi}_{xy} g_{xy} \end{bmatrix}. \quad (32)$$

The determinant of the block matrix in (31) is equal to $\det^2(\hat{I} - \hat{A}(\mathbf{k})) - \psi^4(k) \det^2(\hat{A}(\mathbf{k}))$. Let us write matrix (32) in the form $A_{11} = a(\mathbf{k})$, $A_{12} = b(\mathbf{k})$, $A_{21} = c(\mathbf{k})$, $A_{22} = d(\mathbf{k})$. Then we have DE.

$$\begin{aligned} & [(1 - a(\mathbf{k}))(1 - d(\mathbf{k})) - b(\mathbf{k})c(\mathbf{k})]^2 \\ & - \psi^4(k)(a(\mathbf{k})c(\mathbf{k}) - b(\mathbf{k})d(\mathbf{k})) = 0. \quad (33) \end{aligned}$$

If we are interested in very slow SP, then with a sufficiently large distance d between the sheets $|\psi^4(k)| = |\exp(-2\kappa_z d)| \ll 1$, and DE breaks down into two identical equations:

$$(1 - a(\mathbf{k}))(1 - d(\mathbf{k})) - b(\mathbf{k})c(\mathbf{k}) = 0. \quad (34)$$

They become different with $b(\mathbf{k})=0$ or $c(\mathbf{k})=0$:

$$1 - a(\mathbf{k}) = 0, \quad (35)$$

$$1 - c(\mathbf{k}) = 0. \quad (36)$$

Let us review the opportunity of obtaining them. Let the plasmon move along one of the axes. Then $g_{xy} = 0$. For certainty, let this be the axis x . Then $k_y = 0$, $g_{xx} = \sqrt{k_0^2 - k_x^2}/(2k_0)$, $g_{yy} = k_0/(2\sqrt{k_0^2 - k_x^2})$, meanwhile $b(\mathbf{k}) = \xi_{xy}g_{yy}$, $c(\mathbf{k}) = \xi_{xy}g_{xx}$, therefore, from DE (34) we have $(1 - \xi_{xx}(\mathbf{k})g_{xx}(\mathbf{k}))(1 - \xi_{yy}(\mathbf{k})g_{yy}(\mathbf{k}))^2 + \xi_{xy}^2(\mathbf{k})/4 = 0$. This equation splits into (35) and (36) if the conductivity tensor is reduced to the principal axes, i.e. $\xi_{xy} = 0$. We obtain $1 - \xi_{xx}(\mathbf{k})g_{xx}(\mathbf{k}) = 0$, $1 - \xi_{yy}(\mathbf{k})g_{yy}(\mathbf{k}) = 0$ or $\xi_{xx}(\mathbf{k})k_z(k) = 2k_0$ and $\xi_{yy}(\mathbf{k})k_0^2 = 2k_0k_z(k)$. Squaring them, we have $k_x^2 = k_0^2 - 4k_0^2/\xi_{xx}^2(\mathbf{k})$, $k_x^2 = k_0^2 - \xi_{xx}^2(\mathbf{k})/4k_0^2$. Taking square roots, we obtain two solutions

$$k_x = \pm k_0 \sqrt{1 - 4/\xi_{xx}^2(\omega, \mathbf{k}, T, \mu_c)}, \quad (37)$$

$$k_x = \pm k_0 \sqrt{1 - \xi_{yy}^2(\omega, \mathbf{k}, T, \mu_c)/4}. \quad (38)$$

These are actually implicit equations. The roots with different signs produce waves in two directions. Here we have denoted the dependence of conductivity on all parameters, including chemical potential μ_c . We denote the normalized complex components as $\xi_{xx} = \xi'_{xx} + i\xi''_{xx}$, $\xi_{yy} = \xi'_{yy} + i\xi''_{yy}$. Equation (37) takes the form

$$k_x = \pm k_0 \times \sqrt{\frac{4(\xi_{xx}^{\prime 2} - \xi_{xx}^{\prime\prime 2})}{(\xi_{xx}^{\prime 2} - \xi_{xx}^{\prime\prime 2})^2 + 4(\xi_{xx}^{\prime} \xi_{xx}^{\prime\prime})^2} + \frac{8i\xi_{xx}^{\prime} \xi_{xx}^{\prime\prime}}{(\xi_{xx}^{\prime 2} - \xi_{xx}^{\prime\prime 2})^2 + 4(\xi_{xx}^{\prime} \xi_{xx}^{\prime\prime})^2}}.$$

It shows that for a slow E-SP to exist there should be $\xi_{xx}^{\prime 2} < \xi_{xx}^{\prime\prime 2}$. For a very slow plasmon, $\xi_{xx}^{\prime 2} \ll \xi_{xx}^{\prime\prime 2} \ll 1$ is required, and then

$$k_x \approx \pm k_0 \sqrt{1 + 4/\xi_{xx}^{\prime\prime 2} \left(1 + \frac{4i\xi_{xx}^{\prime}/\xi_{xx}^{\prime\prime} - 8(\xi_{xx}^{\prime}/\xi_{xx}^{\prime\prime})^2}{\xi_{xx}^{\prime\prime 2} + 4} \right)}. \quad (39)$$

The signs \pm correspond to waves in two opposite directions. For slow H-SP there should be $\xi_{yy}^{\prime} \ll |\xi_{yy}^{\prime\prime}|$, $|\xi_{yy}^{\prime\prime}| \gg 1$. In this case,

$$k_x = \pm k_0 \sqrt{1 + (\xi_{yy}^{\prime\prime 2} - \xi_{yy}^{\prime 2} - 2i\xi_{yy}^{\prime} \xi_{yy}^{\prime\prime})/4} \\ \approx \pm k_0 (1 + (\xi_{yy}^{\prime\prime 2} - \xi_{yy}^{\prime 2} - 2i\xi_{yy}^{\prime} \xi_{yy}^{\prime\prime})/8). \quad (40)$$

At low frequencies this SP is almost not decelerated. A stronger deceleration is possible in the $\beta \approx 2\alpha$ region when taking into account SD. From DE (39) it follows that the SP is inverse if the conductivity component is capacitive, i.e. $\xi_{xx}^{\prime\prime} > 0$, and direct if it is inductive. From DE (40) it follows that the SP is inverse if $\xi_{yy}^{\prime\prime} < 0$, i.e. the conductivity component is inductive, and forward — if it is capacitive. Let us review the DE for bonded SP. Let $k_y = 0$ again. Let us denote $X = \sqrt{k_0^2 - k_x^2}/k_0 = \sqrt{1 - n^2}$. As it is easy to see, $X^2 - 2BX + C = 0$, whence $\sqrt{1 - n^2} = B \pm \sqrt{B^2 - C}$, and, squaring, we have a remote control for deceleration

$$n^2 = 1 - \left(B(n) \pm \sqrt{B^2(n) - C(n)} \right)^2. \quad (41)$$

In it

$$B = 1/\xi_{xx} + \xi_{yy} - \xi_{xy}^2/(4\xi_{xx}) \pm \psi^2(k) \sqrt{\xi_{yy}/\xi_{xx} - \xi_{xy}^2/\xi_{xx}^2}/2, \\ C = \xi_{yy}/\xi_{xx}.$$

The signs should be taken independently. When squaring, extra roots could be obtained, which should be taken into account when extracting the root from (41). For $\psi = 0$ and $\xi_{xy} = 0$, (41) naturally implies (37) and (38). DE (41) is implicit, due to the dependence of conductivity on SD and frequency. For such equations, the work [53] proposed an iteration method with correction of the iteration step, based on the implementation of the principle of contraction mappings.

For arbitrary multilayer plane-layered structures, the general method for constructing DE is to match the fields at the boundaries while satisfying the fields in the layers to the wave equations. For homogeneous dielectric layers these are the Helmholtz equations. The fields in them can be represented as a combination of E-waves and H-waves. There may be graphene sheets at the interfaces, which provide a break in the magnetic field components. When taking into account the SD, the sheets are described by a fourth-order matrix $\hat{T}_{\sigma n}$ of type (29). The layer is also described by a fourth-order matrix $\hat{T}(d_n)$ of type (30). The algorithm consists of calculating the complete structure matrix in the form of a product of $\hat{T}(d_n)\hat{T}_{\sigma n}$ matrices and imposing radiation conditions.

5. Numerical results and conclusions

First, we obtain approximate analytical solutions of the DE. We are looking for the roots of equations (37), (38) and (41). We always have the right to choose the x axis along the propagation of the SP. DE (37) and (38) take place only if it coincides with the crystalline axis of graphene. Then it is convenient to write these equations in the form

$$n = k_x/k_0 = \pm \sqrt{1 - 4/\xi_{xx}^2(\omega, n, T, \mu_c)},$$

$$n = k_x/k_0 = \pm \sqrt{1 - \xi_{yy}^2(\omega, n, T, \mu_c)/4},$$

in this case $\sigma_{xy}=0$ and

$$\xi_{xx}(\omega, \omega_c, \mathbf{k}) = \xi^{\text{intra}}(\omega, \omega_c) \left[1 + 3(n/600)^2 \times \left(1 - \frac{2i\omega_c}{3\omega} \right) \right] + \xi^{\text{inter}}(k), \quad (42)$$

$$\xi_{yy}(\omega, \omega_c, \mathbf{k}) = \xi^{\text{intra}}(\omega, \omega_c) [1 + (n/600)^2] + \xi^{\text{inter}}(k). \quad (43)$$

In these formulas, the deceleration is $n < 300$. At $n = 300$, the increase in conductivity reaches 75%, which is no longer a small value and lies beyond the accuracy of these formulas. In reality, for good accuracy, the upper limit of $n = 100$ should be taken. At room temperature and $\mu_e \geq 0.1$ eV the value $\xi^{\text{intra}} = -i\xi_0\alpha/(\pi\beta)$ is very accurate. At $\omega \gg \omega_c$ it has a small real part, i.e. in this case at $n' < 100$ the left parts (42) and (43) — small imaginary negative and decreasing with increasing frequency, therefore the main contribution is at high frequencies gives $\xi^{\text{inter}}(k)$. At optical and UV frequencies, according to formula (14) and its refinements, $\xi^{\text{inter}}(k) \approx \xi_0 \ll 1$, and at normal incidence of a plane wave ($k_z = k_0$, $k_x = 0$), graphene is transparent, and its transmission coefficient $T = 1/(1 + \xi_0/2) = 0.9887$ is close to one.

To obtain the DE in the case of two graphene sheets on both sides of the substrate, it is convenient to use symmetry. The SP in such a structure can be symmetrical or anti-symmetrical. Symmetry can be introduced with respect to any of their field components. Typically, for E-SP, a single transverse magnetic component is taken. We will classify by the magnetic and electric wall in the center of the substrate, which is more convenient. Let us review another conclusion of DE (41). For a magnetic wall, the conductivity is zero. The E-wave of the substrate has a normalized conductivity of $y^e = k_0\varepsilon/\sqrt{k_0^2\varepsilon - k_x^2}$. Transforming it to the graphene

plane, we have $y_{in} + \xi_{xx} = iy^e \tan(\sqrt{k_0^2\varepsilon - k_x^2}d/2) + \xi_{xx}$. We added the conductivity of graphene itself to this. To obtain the DE, we assume $y_{in} + \xi_{xx} = -y_0^e = -k_0/\sqrt{k_0^2 - k_x^2}$, i.e. we equate its vacuum conductivity with a minus sign in accordance with the above remark. Let us review the frequency region where the E-SP is very decelerated ($n^2 \gg n'^2$) with inductive conduction $\xi_{xx} = \xi'_{xx} - i\xi''_{xx}$, $\xi''_{xx} > 0$, with a not too large DP $\varepsilon \sim 1$ and with weak dissipation: $\xi'_{xx} \ll \xi''_{xx}$. For a thick substrate we assume

$$\tan(\sqrt{k_0^2\varepsilon - k_x^2}d/2) = -i \tanh(x) = -i(1 - \delta),$$

$$x = \sqrt{n^2 - \varepsilon}k_0d/2 \approx n'k_0d/2 \gg 1, \quad \delta = 2e^{-2x} \ll 1.$$

We have the DE

$$n \approx \frac{\varepsilon + 1 + (\varepsilon^2 - 1)/2n^2}{\xi'_{xx} + i\xi''_{xx}} (1 - \delta) \quad (44)$$

and its approximate solution $n \approx (2 + \varepsilon)(1/\xi'_{xx} - i\xi''_{xx}/\xi'^2_{xx})$ with $n' \approx (2 + \varepsilon)/\xi''_{xx} \gg 1$ decelerated

since $\xi''_{xx} \ll 1$. DE (44) and its solution were obtained by neglecting terms of the second order of smallness. Let us estimate the maximum deceleration at $\varepsilon = 3$, $\alpha = \sqrt{2}\beta'$ and at zero k . We have $n \approx 80$. Substituting it into (44), we see that the correction is small and equal to $5/(4n^2) \approx 2 \cdot 10^{-4}$. In reality, it may be somewhat less due to the influence of losses. Calculating the correction for SD, we see that it is also small. The solution can be refined by substituting it into (44). From (44) it can be seen that with capacitive conduction the SP — is inverse. Conductivity can become capacitive at high frequencies due to interband contribution. In the absence of a conductive sheet, the method leads to the Zenneck DE $n = \sqrt{\varepsilon/(1 + \varepsilon)}$. Another limiting case of a very small substrate thickness, when $x \ll 1$ and $\tanh(x) = x$, reduces to DE

$$\sqrt{n^2 - 1} = \frac{\xi'_{xx} - k_x\varepsilon d/2 - i\xi''_{xx}}{\xi'^2_{xx} + (\xi'_{xx} - k_0\varepsilon d/2)^2}. \quad (45)$$

If at some frequency the resonance condition $\xi''_{xx}(\omega, \omega_c) = k_0\varepsilon d/2$ is met, then $n = -i\sqrt{1/\xi'_{xx} - 1}$, i.e. E-SP — is highly dissipative. If there is a detuning δ : $\xi''_{xx} - k_0\varepsilon d/2 = \delta\xi'_{xx}$, then with $\delta^2 \gg 1$ we obtain a decelerated E-SP $n \approx 1/(\xi'_{xx}\delta) - i/(\xi'_{xx}\delta^3)$, provided that $\xi'_{xx}\delta < 1$, and the deceleration depends on d . For characteristic frequencies, $k_0\varepsilon d/2 \sim 0.02$ should be satisfied, i.e. at $d = 2$ nm, $\varepsilon = 3$ we have wavelengths $\lambda \sim 830$ nm. Below the frequency of the E-SP transition is direct, and above—reverse. Here there is an analogy with the SP in a thin metal film [17]. For an electric wall, replace the tangent with minus cotangent. For a thick substrate, this practically does not change the DE. For a thin substrate, the SP deceleration is small. In this case we have DE

$$\sqrt{n^2 - 1} = \frac{(\varepsilon - n^2)k_0d/2}{\varepsilon + i\xi_{xx}(\varepsilon - n^2)k_0d/2},$$

and $n' \approx 1$ with $n'' \ll 1$. Substituting these estimates into the DE, we have a refinement

$$n^2 = 1 + [(1 - 1/\varepsilon)k_0d/2 - i\xi_{xx}(1 - 1/\varepsilon)^2(k_0d)^2/4]^2, \quad (46)$$

i.e. the maximum and very small potential deceleration of $n' = 1 + k_0d/4$ will be at a large DP. Both cases are realized when the conductivity transforms from the right to the left graphene sheet. In this case, the resulting differential equation coincides with (41), while by transforming the tangent to the tangent of the half argument, it is transformed to a quadratic equation, both roots of which give two DE for the electric and magnetic walls. For metal film $\varepsilon \approx -\varepsilon'$, therefore the deceleration is greater, the smaller d . The absence of graphene sheets leads to the DE [17] $n = \sqrt{\varepsilon^2\theta^2 - \varepsilon}/\sqrt{\varepsilon^2\theta^2 - 1}$, $\theta = k_0d\sqrt{n^2 - \varepsilon}/2$, which at $\xi_{xx} = 0$ coincides with (45). In a metal film, the maximum deceleration is achieved at $\text{Re}(\varepsilon^2\theta^2) = 1$ and is approximately equal to $n' = \sqrt{1/(k_0^2d^2\varepsilon'\varepsilon'') - \varepsilon'^2/(4\varepsilon'')}$, while $\varepsilon' = \omega_F^2/(\omega^2 + \omega_c^2) - \varepsilon_L$, $\varepsilon'' = \omega_F^2\omega_c/(\omega^3 + \omega\omega_c^2)$,

$\varepsilon_L \sim 10$, $\omega \gg \omega_c$. For SP in graphene sheets on a conductive substrate, there should be $|\varepsilon|k_0d/2 \ll |\xi''_{xx}|$ in the region where $\xi'_{xx} \ll |\xi''_{xx}|$

If we review an asymmetric structure with one graphene sheet, then, transforming from the vacuum conductivity $y_0^e = i/\sqrt{n^2-1}$ to the sheet and further equating the vacuum conductivities with a negative sign, we obtain for E-SP

$$y^e \frac{y_0^e + y^e \tanh(d\sqrt{n^2 - \varepsilon})}{y^e + y_0^e \tanh(d\sqrt{n^2 - \varepsilon})} + \xi_{xx} = -y_0^e,$$

where $y^e = i\varepsilon/\sqrt{n^2 - \varepsilon}$. For a slow SP with inductive conductivity and a large substrate thickness, we replace the hyperbolic tangent with $1-\delta$ and obtain in the first order of smallness in δ and for $n^2 \gg \varepsilon$ the following DE:

$$n = \frac{\varepsilon + 1}{\xi''_{xx}(1 + i\xi'_{xx}/\xi''_{xx}) + \frac{\varepsilon}{n} \frac{\varepsilon-1}{\varepsilon+1} \delta - \frac{\varepsilon^2+1}{2n^3}}$$

$$\approx \frac{\varepsilon + 1}{\xi''_{xx}} (1 - i\xi'_{xx}/\xi''_{xx}).$$

In the case of a very small thickness of the substrate, the DE can be written in the form

$$\sqrt{n^2 - 1} = \left(\frac{1 + \varepsilon}{2} - n^2 \frac{1 + \varepsilon^2}{2\varepsilon} \right) k_0d + \xi''_{xx} (1 + i\xi'_{xx}/\xi''_{xx})$$

$$\times \left[\frac{n^2 - 1}{2} + \frac{n^2 - \varepsilon}{2\varepsilon} \sqrt{n^2 - 1} k_0d \right].$$

Assuming $d = 0$, we obtain

$$\sqrt{n^2 - 1} = (2/\xi''_{xx})(1 - i\xi'_{xx}/\xi''_{xx}),$$

which corresponds to (37). For H-SP on a thin substrate, the DE differs little from (38). For an electrically thick substrate, it is easiest to obtain the DE in the $\delta = 0$ approximation, i.e. for graphene on a dielectric half-space. In this case it looks like $y^h + \xi_{yy} = -y_0^h$, or

$$n^2 = \varepsilon - (\varepsilon - 1 + \xi_{yy}^2)/(4\xi_{yy}^2).$$

If the conductivity is highly reactive, then

$$n^2 \approx \varepsilon + (\varepsilon - 1 - |\xi_{yy}^2|)^2/(4|\xi_{yy}^2|),$$

and SP is low at $\varepsilon > 1 + |\xi_{yy}^2|$. At $\varepsilon = 1$ we obtain DE (38). If deceleration is large:

$$n = \pm(\varepsilon - 1)/\sqrt{\xi_{yy}^2 - \xi_{yy}^2} (1 - i\xi'_{yy}\xi''_{yy}/(\xi_{yy}^2 - \xi_{yy}^2))/2.$$

In the region of low losses $n' \approx \pm(\varepsilon-1)/(2\xi_{yy}^2)$, i.e., using a thick substrate with a large DP can lead to a slow H-SP. At $\varepsilon = 3$, $\alpha = \beta'$ we have $\xi_{yy}^2 = \xi_0\alpha/(\pi\beta') = 0.007$, $n' = 143$. With such a deceleration, the influence of SD is still small. However, changing the parameters can lead to an increase in ξ_{yy}^2 , i.e. to a limitation of deceleration, as for the E-SP. For H-SP on a very thin substrate, the DE differs

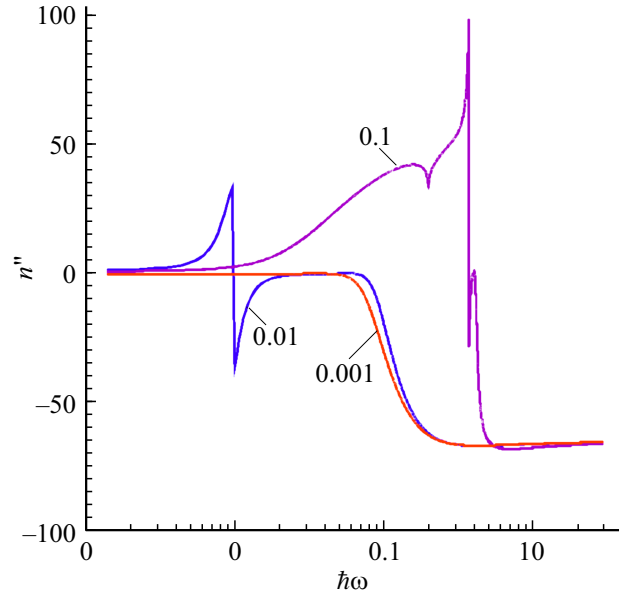


Figure 3. Dependence of losses $n'' = k_x''/k_0$ on $\omega\hbar$ (eV) for E-plasmon at different values of chemical potential (eV), $\omega_c = 10^{12}$ GHz.

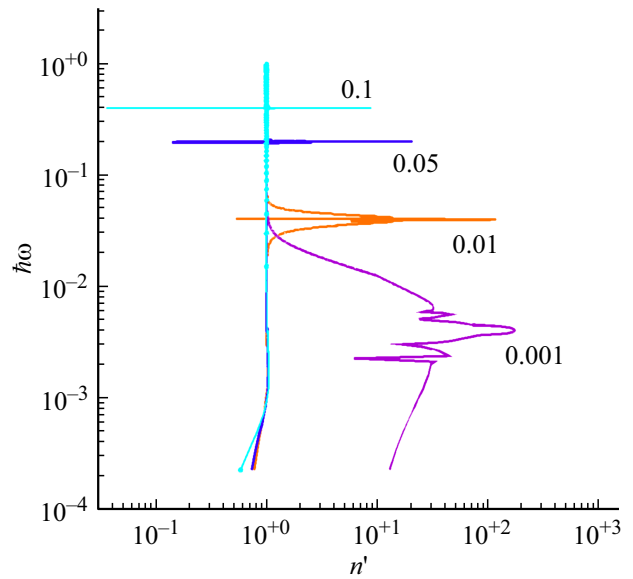


Figure 4. H-plasmon dispersion (dependence of $\omega\hbar$, eV, on deceleration) at different values of the chemical potential (shown in eV), $\omega_c = 10^{12}$ GHz.

little from (38), i.e. $n \approx 1$. The effect of a thin substrate can be considered by introducing its normalized surface conductivity $\xi_d = ik_0d(\varepsilon-1)$. It works if $k_0d\sqrt{\varepsilon} \ll 1$. In this case, $\xi_d + \xi_{yy} = -y_0^h$, i.e., the capacitive conductivity of the substrate reduces the inductive conductivity of the sheet and the deceleration.

The dependences of the normalized conductivity on the deceleration, calculated using various formulas, are given in the table. Figures 2 and 3 show the results of iterative calculation of the E-SP dispersion (37) for different

Dependence of conductivity ξ_{xx} on deceleration n' : according to formulas (15), (20) and (22); based on formula (15) in the numerical calculation of integral (11); based on the calculation of integrals (5) and (11). $\omega_c = 10^{12}$ Hz, $n'' = n'$

Deceleration n'	$\alpha = 5, \beta' = 5$					
	(15), (20)		(15), (11)		(5), (11)	
	ξ'_{xx}	ξ''_{xx}	ξ'_{xx}	ξ''_{xx}	ξ'_{xx}	ξ''_{xx}
1	0.022580	-0.027792	0.02286	-0.027706	0.02891	-0.027678
10	0.022567	-0.027679	0.02528	-0.028094	0.02552	-0.027819
100	0.021202	-0.027681	0.02809	-0.050388	0.02864	-0.048015
$\alpha = 5, \beta' = 10$						
1	0.0478122	11.26550	0.085391	11.302668	0.085382	11.30263
10	0.0478190	11.26551	0.492861	11.634970	0.025527	11.63484
100	0.0485013	11.26552	11.42283	10.409300	0.028646	10.40812
$\alpha = 10, \beta' = 5$						
1	0.028555	-0.017617	0.028902	-0.017858	0.028382	-0.017809
10	0.028531	-0.017618	0.028613	-0.018908	0.030873	-0.018418
100	0.026191	-0.017764	0.025701	-0.477282	0.026671	-0.043502

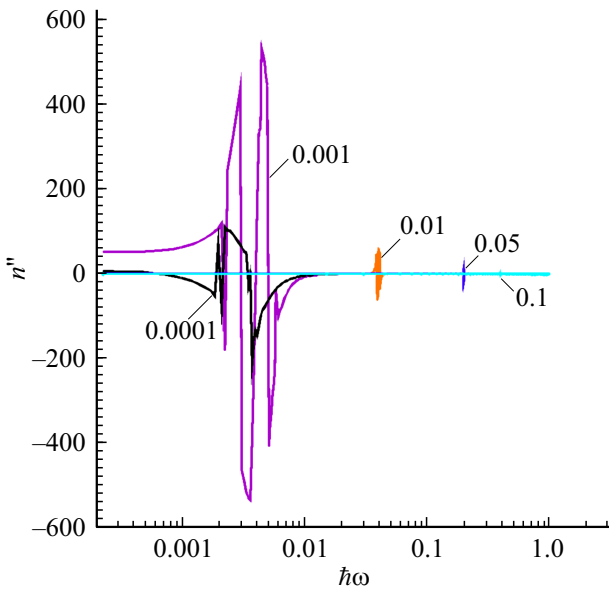


Figure 5. Losses $n'' = k''_x/k_0$ of H-plasmon depending on $\omega\hbar$ (eV) at different values of the chemical potential (eV), $\omega_c = 10^{12}$ GHz.

values of the chemical potential up to the optical range, and Figs 4, 5 — show similar results for H-SP (38). All the figures are constructed in such a way that $\text{Re}(n) = n' > 0$ (the direction of phase motion is taken everywhere as the positive direction), therefore negative losses $n'' = -\text{Im}(n)$ mean reverse SP. In Figs. 3 and 5, the losses change sign on the spectral lines, and several such changes are possible (Fig. 5). The iterations for all the results con-

verged well enough that no special methods for improving convergence had to be applied [53]. It should be noted that for dissipative plasmons, the decreasing portion of the dispersion characteristic (negative group velocity) does not mean that the SP is inverse. In both the decreasing and increasing sections of the dispersion curves, a transition from direct to reverse SP is possible. H-SP does not interact with electron beams in the direction of motion, therefore E-SP [18] are promising for THC electronics. In the optical and near-UV ranges, E-SP are highly dissipative, which is associated with almost real conductivity, but decelerated. A slow plasmon is a quantum quasiparticle with a fairly large momentum $p = \hbar k_0 n'$ compared to the momentum of a photon. Therefore, for a SP it is more likely to observe the Compton effect of electron scattering on it. The given formulas work up to photon energies $\hbar\omega = \gamma_0 = 2.8$ eV, when the π bonds are broken. Above, the 2D plasma conductivity model can be applied. An increase in SP deceleration is associated with a decrease in losses. In this regard, the application of cryogenic temperatures for graphene is inappropriate. More promising is the application of optical pumping [9–12].

Acknowledgments

The work was supported by the Ministry of Science and Higher Education of the Russian Federation as part of the State Assignment (№FSRR-2023-0008).

Conflict of interest

The author declares that he has no conflict of interest.

References

- [1] S. Mikhailov, K. Ziegler. *Phys. Rev. Lett.*, **99**, 016803 (2007). DOI: 10.1103/PhysRevLett.99.016803
- [2] G.W. Hanson. *J. Appl. Phys.*, **103**, 064302 (2008). DOI: 10.1063/1.2891452
- [3] G.W. Hanson. *J. Appl. Phys.*, **104**, 084314 (2008). DOI: 10.1063/1.3005881
- [4] P.I. Buslaev, I.V. Iorsh, I.V. Shadrivov, P.A. Belov, Yu.S. Kivshar. *Pisma v ZhETF*, **97**(9), 619 (2013) (in Russian). DOI: 10.7868/S0370274X1309008
- [5] K.J.A. Ooi, D.T.H. Tan. *Proceed. Royal Society A*, **473**, 20170433 (2017). DOI: 10.1098/rspa.2017.0433
- [6] Yu.V. Bludov, A. Ferreira, N.M.R. Peres, M.I. Vasilevskiy. *Intern. J. Modern Phys. B*, **27**(10), 1341001 (2013). DOI: 10.1142/S0217979213410014
- [7] X. Luo, T. Qiu, W. Lum, Z. Ni. *Mater. Sci. Eng. R.*, **MSR-434**, 1 (2013). DOI: 10.1016/j.mserr.2013.09.001
- [8] M. Jablan, M. Soljačić, H. Buljan. *Proc. IEEE*, **101**(7), 1689 (2013). DOI: 10.1109/JPROC.2013.2260115
- [9] V. Ryzhii, A.A. Dubinov, T. Otsuji, V. Mitin, M.S. Shur. *J. Appl. Phys.*, **107**, 054505 (2010). DOI: 10.1063/1.3327212
- [10] V. Ryzhii, I. Khmyrova, M. Ryzhii, A. Satou. *Int. J. High Speed Electron. Systems*, **17**(03), 521 (2007). DOI: 10.1142/S0129156407004710
- [11] V. Ryzhii, A. Satou, T. Otsuji. *J. Appl. Phys.*, **101**, 024509 (2007). DOI: 10.1063/1.2426904
- [12] V. Ryzhii. *Jpn. J. Appl. Phys.*, **45**(35), L923 (2006). DOI: 10.1143/JJAP.45.L923
- [13] G.W. Hanson. *IEEE Trans. Antennas Propag.*, **56**(3), 747 (2008). DOI: 10.1109/TAP.2008.917005
- [14] G.O. Abdullaev, Z.Z. Alisultanov. *FTT*, **61**(3), 618 (2019) (in Russian). DOI: 10.21883/FTT.2019.03.47260.289
- [15] J. Nilsson, A.H. Castro Neto, F. Guinea, N.M.R. Peres. *Phys. Rev. Lett.*, **97**, 266801 (2006). DOI: 10.1103/PhysRevLett.97.266801
- [16] L.A. Vainshtein. *Elektromagnitnye volny* (Radio i Svyaz', M., 1988) (in Russian).
- [17] M.V. Davidovich. *Kvantovaya elektronika*, **47**(6), 567 (2017) (in Russian). DOI: 10.1070/QEL16272
- [18] M.V. Davidovich. *Proc. SPIE*, **11066**, 1106614 (2019). DOI: 10.1117/12.2521234
- [19] V. Ryzhii, A.A. Dubinov, T. Otsuji, V. Mitin, M.S. Shur. *J. Appl. Phys.*, **107**, 054505 (2010). DOI: 10.1063/1.3327212
- [20] V. Ryzhii, I. Khmyrova, M. Ryzhii, A. Satou. *Int. J. High Speed Electron. Systems*, **17**(03), 521 (2007). DOI: 10.1142/S0129156407004710
- [21] V. Ryzhii, A. Satou, T. Otsuji. *J. Appl. Phys.*, **101**, 024509 (2007). DOI: 10.1063/1.2426904
- [22] V. Ryzhii. *Jpn. J. Appl. Phys.*, **45**(35), L923 (2006). DOI: 10.1143/JJAP.45.L923
- [23] E.H. Hwang, S. Das Sarma. *Phys. Rev. B*, **75**, 205418 (2007); **80**, 205405 (2009). DOI: 10.1103/PhysRevB.75.205418
- [24] V. Despoja, D. Novko, K. Dekanic, M. Sunjić, L. Marusić. *Phys. Rev. B*, **87**, 075447 (2013).
- [25] M.A.K. Othman, C. Guclu, F. Capolino. *AP-S*, **2013**, 484 (2013).
- [26] M. Othman, C. Guclu, F. Capolino. *Opt. Express*, **21**(6), 7614 (2013). DOI: 10.1364/OE.21.007614
- [27] M. Jablan, M. Soljačić, H. Buljan. *Proc. IEEE*, **101**(7), 1689 (2013). DOI: 10.1109/JPROC.2013.2260115
- [28] J.S. Gomez-Diaz, M. Tymchenko, A. Alú. *Opt. Mater. Express*, **5**, 2313 (2015). DOI: 10.1364/OME.5.002313
- [29] J.S. Gomez-Diaz, A. Alu. *Graphene-Based Hyperbolic Metasurfaces*, 2016 10th Europ. Conf. Antennas and Propagation (EuCAP) (Davos, Switzerland, 2016), p. 1–4. DOI: 10.1109/EuCAP.2016.7481165
- [30] J.S. Gomez-Diaz, M. Tymchenko, A. Alú. *Phys. Rev. Lett.*, **114**, 233901 (2015). DOI: 10.1103/PhysRevLett.114.233901
- [31] D. Correas-Serrano, J.S. Gomez-Diaz, M. Tymchenko, A. Alú. *Opt. Express*, **23**(23), 29434 (2015). DOI: 10.1364/OE.23.029434
- [32] Z. Guo, H. Jiang, H. Chen. *J. Appl. Phys.*, **127**, 071101 (2020). DOI: 10.1063/1.5128679
- [33] M.V. Davidovich. *Komp. opt.*, **45**(1), 48 (2021) (in Russian). DOI: 10.18287/2412-6179-CO-673
- [34] M.V. Davidovich. *UFN* **189**(12), 1250 (2019) (in Russian). DOI: 10.3367/UFNr.2019.08.038643
- [35] P.M. Platzman, P.A. Wolff. *Volny i vzaimodeystviya v plazme tverdogo tela* (Mir, M., 1975) (in Russian).
- [36] V.N. Konopsky, E.V. Alieva. *Phys. Rev. Lett.*, **97**, 253904 (2006). DOI: 10.1103/PhysRevLett.97.253904
- [37] P. Berini. *Adv. Opt. Phot.*, **1**(3), 484 (2009). DOI: 10.1364/AOP.1.000484
- [38] Y. Wang, E.W. Plummer, K. Kempa. *Adv. Phys.*, **60**(5), 799 (2011). DOI: 10.1080/00018732.2011.621320
- [39] A. Norrman, T. Setälä, A.T. Friberg. *Opt. Lett.*, **38**(7), 1119 (2013). DOI: 10.1364/OL.38.001119
- [40] A.A. Orlov, A.K. Krylova, S.V. Zhukovsky, V.E. Babicheva, P.A. Belov. *Phys. Rev.*, **A90**, 013812 (2014). DOI: 10.1103/PhysRevA.90.013812
- [41] A. Delfan, I. Degli-Eredi, J.E. Sipe. *J. Opt. Soc. Am. B*, **32**, 1615 (2015). DOI: 10.1364/JOSAB.32.001615
- [42] F. Chiadini, V. Fiumara, A. Scaglione, A. Lakhtakia. *J. Opt. Soc. Am.*, **B33**(6), 1197 (2016). DOI: 10.1364/JOSAB.33.001197
- [43] L.A. Falkovsky, A.A. Varlamov. *Eur. Phys. J. B*, **56**, 281 (2007). DOI: 10.1140/epjb/e2007-00142-3
- [44] V.P. Gusynin, S.G. Sharapov, J.P. Carbotte. *Phys. Rev. Lett.*, **96**, 256802 (2006).
- [45] P.R. Wallace. *Phys. Rev.*, **71**, 622 (1947).
- [46] K. Ziegler. *Phys. Rev. Lett.*, **97**, 266802 (2006).
- [47] S. Das Sarma, S. Adam, E.H. Hwang, E. Rossi. *Rev. Mod. Phys.*, **83**, 407 (2011).
- [48] A.H. Castro Neto, F. Guinea, N.M.R. Peres, K.S. Novoselov, A.K. Geim. *Rev. Mod. Phys.*, **81**(1), 109 (2009).
- [49] V.P. Gusynin, S.G. Sharapov, J.P. Carbotte. *Phys. Rev. B*, **75**, 165407 (2007). DOI: 10.1103/PhysRevB.75.165407
- [50] T. Stauber, N.M.R. Peres, A.K. Geim. *Phys. Rev. B*, **78**, 085432 (2008). DOI: 10.1103/PhysRevB.78.085432
- [51] G. Lovat, G.W. Hanson, R. Araneo, P. Burghignoli. *Phys. Rev. B*, **87**, 115429 (2013). DOI: 10.1103/PhysRevB.87.115429
- [52] D.W. Berreman. *J. Opt. Soc. Am.*, **62**(4), 502 (1972).
- [53] M.V. Davidovich, A.K. Kobets, K.A. Sayapin. *Fizika volnovykh protsessov i radiotekhnicheskiye sistemy*, **24**(3), 18 (2021) (in Russian). DOI: 10.18469/1810-3189.2021.24.3.18

Translated by A.Akhtyamov